Published by The College of Vocational and Technology Education (COVTED), TASUED, vol. 20, no 1, pp. 58-68

COVTED, TASUED
The Vocational and Applied Science Journal (VAS)

Multiscale Nonlinear Analysis of AE and AU Geomagnetic Activity Indices during the 2014 Solar Maximum

[1]Adelaja, A. D., [1]Bamidele, K. J., [2]Kotoye, A. A., [1]Fowodu., T. O., [1]Fagbohun, M. A., and [1]Falayi. E. O.
[1]Department of Physics, Tai Solarin Federal University of Education, Ijagun, P.M.B. 2118 Ijebu-Ode, Ogun State, Nigeria
[2]Department of Science Laboratory Technology, Abraham Adesanya Polytechnic, Ijebu Igbo, Ogun State, Nigeria
Corresponding email: *ayodeleenochadelaja@gmail.com*

Abstract
This study investigates the variability and chaoticity behaviour of hourly geomagnetic field parameters (Auroral Electrojet and Upper Auroral Electrojet) data from January 1st – December 31st 2014, corresponding to peak solar activity obtained from the OMINIWEB dataset. Nonlinear time series techniques such as Embedding Taken's and Wavelet Power Spectrum analysis were applied to reconstruct the hidden system dynamics and energy distribution respectively. Analysis of AE and AU indices exhibited similar irregular and highly fluctuating patterns particularly during geomagnetic disturbances. Embedding Taken's showed that delay time τ = 12 and embedding dimension m = 7 for both indices, these values were used for phase space reconstruction. Computed Largest Lyapounov Exponent (LE) with value 0.152 for AE index and 0.132 for AU index (positive values) indicate the presence of deterministic chaos within the geomagnetic system. Hurts exponent analysis revealed that AU and AE indices displayed values of 0.96 and 0.78 respectively corresponding to perfectly deterministic process with strong persistence. The Wavelet Power Spectrum (WPS) analysis indicated significant energy concentrations, with average value of approximately 16,000mm^2 for AE and 60,000mm^2 for AU, confirming strong temporal variability in both indices. Overall, the results demonstrated that temporal evolution of AE and AU indices are governed by an underlying chaotic dynamics; behaviour arising from the complex interaction between solar wind conditions, magnetotail energy storage processes, and ionospheric current dynamics capable of triggering geomagnetic storms which enhances system instability. This study therefore provides valuable insight into nonlinear dynamics of geomagnetic activity during periods of intense solar forcing.

Keywords: Auroral Electrojet, Lyapounov Exponent, Hurst Exponent, Wavelet Power Spectrum, Nonlinear Time Series.

1. Introduction

The Earth's geomagnetic field represents a fundamental component of the near-Earth space environment, serving as the primary protective shield against solar wind and cosmic radiation. The magnetosphere is the outermost portion of the Earth's magnetic field into space, which is generated by dynamo processes in the liquid outer core, a region where the Earth's magnetic field dominates over the interplanetary magnetic field. Understanding the dynamics and variability of geomagnetic field parameters has become increasingly critical in the modern technological era, where Space weather phenomena may possess some significant impacts on communication networks, satellite operations, power grids, and navigation technologies (Kivelson *et al*., 1996; Ishii *et al.*, 2024).

Geomagnetic activity indices provide quantitative measures of Earth's magnetic field disruptions brought about by solar-terrestrial interactions. Among these indices, the auroral electrojet (AE) indices constitute one of the most widely utilized sets of parameters for monitoring and characterizing magnetospheric substorm activity. The AE index family comprises four distinct indices: AE (auroral electrojet), AU (auroral upper envelope), AL (auroral lower envelope), and AO (auroral average), each providing unique information about current systems flowing in the auroral ionosphere between approximately 60° and 70° geomagnetic latitude (Davis & Sugiura, 1966; Rostoker, 1972; Nakamura *et al.*, 2015).

The AU index specifically represents the maximum positive deviation of the geomagnetic field's horizontal component from quiet-day values at auroral zone observatories. This index primarily reflects the intensity of the eastward electrojet current flowing in the dusk sector of the auroral oval during geomagnetic disturbances. The AU index provides critical information about energy deposition processes in the magnetosphere-ionosphere system and serves as an important indicator of the magnetosphere's response to solar wind driving (Kamide *et al*., 1998; Sarris, 2019).
Numerous studies on the application of chaos

Adelaja, A. D., Bamidele, K. J., Kotoye, A. A., Fowodu., T. O., Fagbohun, M. A., and Falayi. E. O., (2026). Multiscale Nonlinear Analysis of AE and AU Geomagnetic Activity Indices during the 2014 Solar Maximum. *The Vocational and Applied Science Journal (VAS)*, vol. 20, no. 1, pp. 58-68.

techniques for quantifying nonlinear variability in time-series data had been conducted in the past (Unnikrishnan, 2008; Rabiu *et al*. 2015; Alves *et al*., 2017; Suresh and Selvaraj, 2017; Riabova, 2018; Falayi *et al*., 2019; Ambika and Harikrishnan , 2019; Falayi *et al.,* 2020; Adelaja *et al.,* 2021; Bamidele *et. al*, 2025a). When applied to geomagnetic field parameters, nonlinear time series analysis can reveal hidden dynamical structures which can identify deterministic chaos, characterize system complexity and also detect precursors to extreme events (Zbilut and Webber, 1992; Mallat, 1999; Schreiber and Kantz, 1995).

The study of dynamical systems with chaotic behaviour and their routes to chaos was in particular attention at recent years (Adelaja *et al.,* 2024). These phenomena study in a non-smooth dynamical system is of the special interest to researchers. Wavelet Transform is a technique used to investigate the intermittent route to chaos, boundary crisis, and transitional regimes under quasi-periodic route to chaos in strongly nonlinear non-smooth discontinuous 2-DOF vibro-impact system (Chen *et al.,* 2011).

Wavelet power spectrum is a technique for estimating the frequency of events in proportion to their location within a time series. The concept of the wavelet power spectrum is employed in coherent structures in turbulent flows (Farge, 1992) and in ionospheric and magnetospheric investigations of the atmosphere (Meyers *et al*., 1993). Understanding the dynamical transitions and characterizing the nonlinear properties of geomagnetic indices such as AE and AU can provide fundamental insights into magnetospheric energy transfer mechanisms and substorm physics (Vassiliadis *et al.*, 1995a; Wanliss, 2005). This study therefore aims to provide new insights into the dynamical characteristics of auroral electrojet systems and also contribute to improved understanding of magnetospheric substorm processes by employing multiple complementary nonlinear techniques and with further examination of the extended datasets covering various geomagnetic activity conditions.

In this research, geomagnetic field parameters, specifically the AE and AU indices were analyzed using nonlinear time series and wavelet power spectrum techniques to reveal the hidden structure through phase space reconstruction, quantify the chaocity of the geomagnetic field parameters and then evaluate the energy distribution of the dynamics

2.0 Materials and Methods

2.1 Data Collection

The Flight Center Space Physics Data Facility (GSFC/SPDF) OmniWeb (http://omniweb.gsfc.nasa.gov) interface geomagnetic (AU and AE) indices hourly data from January 1st to December 31st, 2014 for the year of solar maximum due to an increase in sunspot and solar activity were obtained and used for this study.

2.2 Methods

Analyzing the chaoticity of these geomagnetic field parameters time series, nonlinear techniques Embedding Taken’s was used for Phase Space Reconstruction. Average Mutual Information (AMI) and False Nearest Neighbor (FNN) were adopted for the choice of appropriate delay time τ and embedding dimension m. In order to quantify the chaos in geomagnetic field parameters, Lyapounov Exponent (LE) was computed. Wavelet Power Spectrum (WPS) technique was employed to evaluate the energy distribution while Hurst Exponent was also applied analyse the level of determinism of the geomagnetic field parameters time series.

2.2.1 Phase Space Reconstruction

Average Mutual Information (AMI)

Fraser and Swinney (1986) developed a technique to determine time delayed coordinates that are as independent from one another as possible in order to estimate the ideal time delay for embedding a one-dimensional time series. The mutual information between the original and transformed time series was employed to quantify dependence. Mutual information is referred to as average mutual information (AMI) or auto mutual information since it is calculated for both a time series and a time-shifted version of the same time series. Equation (1) gives the mathematical expression of predictable of AMI technique.

$$Q = -\sum I_{kl(\tau)\ln\frac{I_{kl}(\tau)}{I_{kl}}} \quad (1)$$

where I_k is the probability of obtaining a time series value in the interval, and k and $I_{kl}(\tau)$ are the combined probabilities that a time series value can be acquired in segment k at time t and I at time t + τ. The time delay (τ) is defined as the first lowest value of Q for various locations (Fraser and Swinney, 1986; Kennel *et al.,* 1992; Hirata *et al.,* 2006; Vlachos and Kugiumtzis, 2009; Adelaja *et al.,* 2021).

False Nearest Neighbors (FNN)

The false nearest neighbors (FNN) is applied to a univariate data in order to reconstruct its phase space geometry by embedding its dimension and eliminating the unfitting neighbors. Along the process, FNN changes as the embedding dimension gets more intense. The points in a dimension are close to one another due to prediction; this will be separated into upper dimensions. The difference between two relative distance neighbor points gets wider as one advances from d to d +1, and it can be used as a degree for casting embedding errors. This technique has been utilized by several researchers (Kennel *et al.,* 1992; Adewole *et al.,* 2020; Falayi *et al.,* 2024). In this study, false nearest neighbors (FNN) was applied to determine the embedding dimension of the geomagnetic field indices AE and AU. Equation (2) gives the expression for the false nearest neighbor distance.

$$\left[\frac{X^2{}_{d+1}(t,r)-X^2{}_d(t,r)}{X^2{}_d}\right]^{\frac{1}{2}}=\left[\frac{y(t+r)-y(t_\tau+\tau)}{X_d}\right]\succ X_{tot} \quad (2)$$

where t and t_r, respectively, stand for neighbor and origin points. In the phase space reconstruction with embedding dimension, X_d stands for distance. The tolerance threshold is indicated by X_{tot}.

In time series data analysis, space phase reconstruction with embedding dimension (m) and time delay (τ) are required to acquire the dynamical properties (space geometry) of such system (Takens, 1981). The relationship between delay time τ and embedding dimension m is expressed in Equation (3).

$$P(t)=\left(x_t, x_{t-\tau}, x_{t-2\tau}\ldots\ldots\ldots\ldots x_{t-(m-1)\tau}\right) \quad (3)$$

where *m* and τ is the embedding dimension and delay time respectively.

2.2.2 Chaotic Quantifier (Lyapunov Exponent)

Lyapunov exponent is chaotic quantifier that measures divergence or convergence rate of the near trajectories. The presence of chaos in a dissipative deterministic system is indicated by a positive Lyapunov exponent showing the divergence of the nearby trajectories (Eckman and Ruelle 1985; Ogunsua *et al.,* 2014; Falayi *et al.,* 2020). The rate of divergence as estimated by Abarbanel and Lali (1996) can be determined using equation 4.

$$\lambda=\lim\frac{1}{n}\ln\frac{\left|\Delta x(\chi_o,n)\right|}{\left|\Delta\,\chi_o\right|} \quad (4)$$

where λ denotes Lyapunov exponents (LE), which are used to differentiate between various path patterns and compute the rate of divergence.

Equation (5) depicts the largest Lyapunov exponent which is an accurate estimation of a chaotic dynamical structure (Abarbanel and Lali, 1996).

$$\Delta_n=\frac{1}{\lambda_{\max}} \quad (5)$$

2.2.3 Hurst Exponent

The Hurst exponent was developed by Harold Edwin Hurst as an approach for determining the predictability of a time series is (Hurst, 1951; Mitra, 2012). It indicates how previous values affect future behaviour over a range of times. It is a conventional technique for identifying long memory or persistence in a time series. Hurst exponent has been applied in numerous fields and is utilized not only as a measure of long-term memory but also to correlate the fractal dimension of the time series.

The Hurst exponent H is a statistical measure used to characterize the long-term memory and persistence properties of a time series, with values constrained within the interval $0\leq H\leq 1$. A value of $H=0.5$ corresponds to a purely random process which is analogous to a classical Brownian motion or random walk, suggesting the absence of temporal correlation. The time series will display extreme anti-persistence with successive values alternating direction at each step when H= 0 but when $0\leq H\leq 0.5$, the time series exhibits anti-persistent (or mean-reverting) behavior. This implies that successive increments are negatively correlated. In this regime, increments are more likely to be followed by decrement, and vice versa; indicating that existing trends are unlikely to persist. However, the time series demonstrates persistent behaviour, characterised by positive long-range dependence when $0.5\leq H\leq 1$. In this case, increases are likely to be followed by further increases, indicating that the prevailing trend tends to continue over time. In a situation where the value of H=1, this corresponds to a perfectly deterministic process with strong persistence (Gómez-Águila *et al.,* 2022; Balasis et al., 2023).

Hurst exponent has been successfully applied to ionospheric phenomenal (Nikolopoulos *et al*., 2019; Momeni and Migoya-Orué, 2025). High Hurst exponent value in ionospheric studies reveals the presence of long-range correlations where space weather effects like solar flares or geomagnetic storms last for a long time, while a low Hurst exponent value shows a non-persistent behavior. This is important as it enables distinction between chaotic and turbulence processes in the plasma (Albert *et al.,* 2021; Sierra-Porta *et al*., 2024). The Hurst exponent is obtained using R/S analysis.

$$\left(\frac{R}{S}\right)_n\approx C_n\,H \quad (6)$$

$$Log\left(\frac{R}{S}\right)_n=Log\,C+H\,Log\,n \quad (7)$$

where H is the Hurst exponent.

2.2.4 Wavelet Power Spectrum

The wavelet power spectrum is a technique for estimating the frequency of events in proportion to their location within a time series. The non-analytic Morlet wavelet, a function with a single parameter, was used to obtain the results that were displayed in equation (8).

$$\psi_{a,b(t)}\;=\;a^{1/2}\psi\left(\frac{t-b}{a}\right) \quad (8)$$

where a represents the scale associated with the wavelet's increase and decrease and b depicts the localization of time Morlet wavelet is expressed in equation (9) as (Torrence and Compo, 1998).

Published by The College of Vocational and Technology Education (COVTED), TASUED, vol. 20, no 1, pp. 58-68

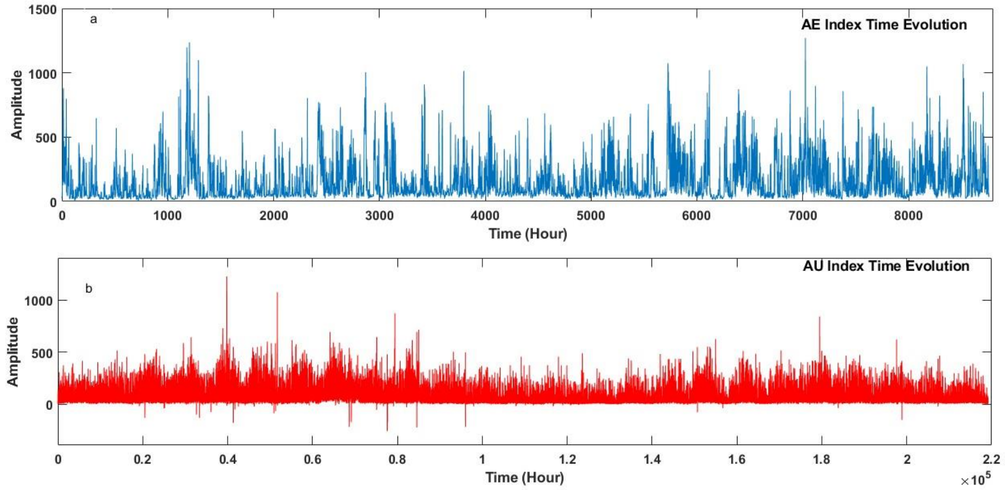

Figure 1: Time evolution of solar maximum of the geomagnetic parameters dynamics from January 1st to December 31st, 2014 *(a) AE; (b) AU*.

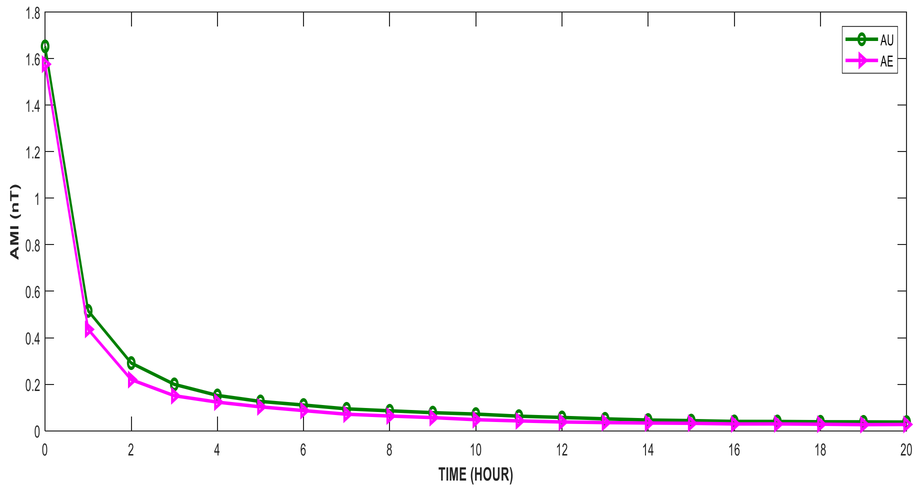

Figures 2: Average mutual information in bits against the delay time in hour obtained for AU and AE during the solar maximum of the geomagnetic parameters from January 1st to December 31st, 2014.

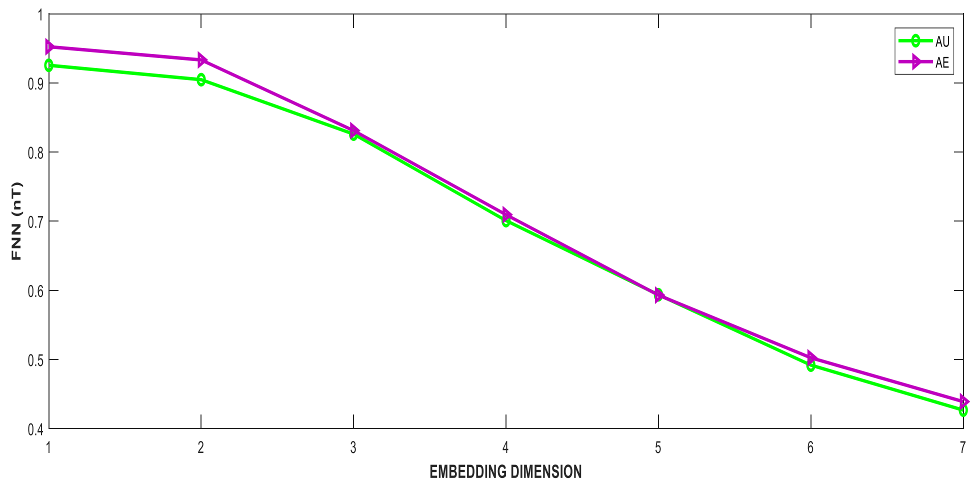

Figures 3: Variation of False nearest neighour against embedding dimension for AE and AU during the solar maximum from January 1st to December 31st, 2014.

$$\psi_{(t)} = \frac{e^{i\omega_o t}}{\sqrt[4]{\pi e^{\frac{t^2}{2}}}} \qquad (9)$$

where ω_o is the non – dimensional frequency parameter of equation (10) (Riabova, 2018; Falayi *et. al.*, 2020)

$$wps_{(a,b)} = \int_{-\infty}^{\infty} x(t)\psi^{*}a, b\,(t)dt \qquad (10)$$

where, $\psi_{a,b}{}^{*}(t)$ denoted as the conjugate of wavelet function $\psi_{a,b}(t)$.

The time series of the data of Morlet wavelet is presented in equation (11) as suggested by Falayi *et. al.,* (2020). The expression of the wavelet coefficient at time index n' and scale a, is also expressed in equation (11).

$$wps_n(a) = \sum_{n'=0}^{N-1} x((n')\psi^{*}\left[\frac{(n'-n)dt}{a}\right] \qquad (11)$$

3.0 Results and Discussion

3.1 Results

3.1.1 Geomagnetic Parameters (AE & AU) Temporal Variability

In an attempt to examine the dynamics of geomagnetic parameters (AE and AU), temporal variability of system is carried out. Figures 1(a – b) shows the time series for the AU and AE indices, a significant degree of changes in the point plot's variability indicates that the system does not exhibit any consistent patterns and as such there is no serious pronouncement of any periodicity in the system.

3.1.2 Phase Space Reconstruction

The variations of geomagnetic field indices AE and AU dynamics as observed in Figure 1 makes accurate description of AE and AU internal dynamics difficult to predict. In order to reveal the internal dynamics of the systems, it is crucial to apply a nonlinear approach like Embedding Taken's for appropriate reconstruct of their phase space (attractors).

Determination of delay time by Average Mutual Information (AMI)

To reconstruct the attractor of AU and AE indices, equation (1) is applied with appropriate value of τ which is obtained at the first minimum of AMI (Fraser and Swinney, 1986; Kennel *et al.*, 1992; Hirata *et al.*, 2006; Vlachos and Kugiumtzis, 2009; Adelaja *et al.*, 2021).

The variation plot of Average Mutual Information (AMI) against the delay time τ for AU and AE indices as shown in Figure 2 with the choice of appropriate delay time τ = 12.

Determination of False Nearest Neighour (FNN)

In this study, false nearest neighbors (FNN) was applied to determine the embedding dimension of the geomagnetic field indices AE and AU using Equation (2). Figure 3 shows the variatons of False nearest neighour with embedding dimension as computed for AE and AU. The Figure shows that the choice of embedding dimension m = 7 will be sufficient being the first minimum point.

For the AE (auroral electrojet) and AU (Upper Auroral Electrojet) during the said solar maximum year, the space phase reconstruction with embedding dimension (m = 7) and time delay (τ = 12) are required to acquire the precise dynamical properties (space geometry) of the system (Takens, 1981) Figures 4(a-b) and 5(a-b) are the phase space reconstruction of the geomagnetic parameters AE and AU respectively for the solar maximum from January 1st to December 31st, 2014.

Chaotic Quantification of the AU and AE Indices

For characterization of the chaoticity of *AU and AE Indices* dynamics, AU and AE values from January through December 2014, the Lyapunov exponent was calculated. The derived Lyapunov exponent was calculated using embedding dimension = 12 and delay m = 7. The values of AU and AE are displayed in Figure 6.

To further understand the dynamics of geomagnetic parameters (AE and AU), Hurst exponent of system is carried out. Figure7 (a – b) shows the Hurst exponent analysis for the AU and AE indices respectively.

Analysing the energy distribution of geomagnetic parameters (AE and AU) during the solar maximum as a time-frequency behaviors, wavelet Power Spectrum analysis was conducted on geomagnetic parameters during the solar maximum. Figures 8(a – b) show the evaluation of the wavelet power spectrum of AE and AU indices time-frequency behaviors

Figure 8: Wavelet Power Spectrum for geomagnetic parameters during the solar maximum from January 1st to December 31st, 2014 (a) AE and (b) AU

3.2 Discussions

The initial investigation of the AE and AU time series reveals highly variable and irregular patterns characterized by frequent bursts of intense activity interspersed with quieter intervals. These fluctuations are typical of geomagnetic environments where the magnetosphere is constantly driven by variable solar wind conditions and internal magnetospheric dynamics. The AE index shows multiple sharp peaks reaching 300–600 nT, signifying strong enhancements of the westward electrojet during magnetospheric substorm activity, as illustrated in Figure 1(a). Meanwhile, the AU index displays even broader fluctuations, with several surges between 400–800 nT, reflecting eastward electrojet intensification associated with dayside reconnection processes, as shown in Figure 1(b).

a

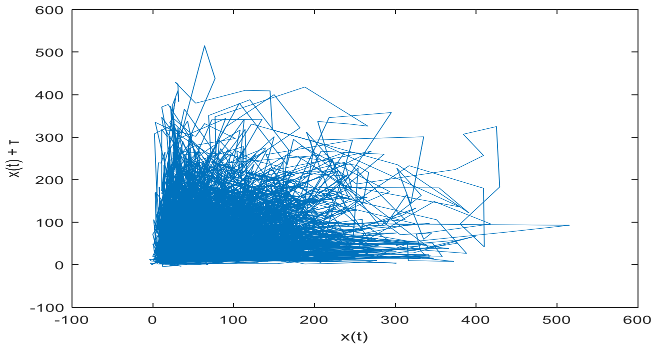

b

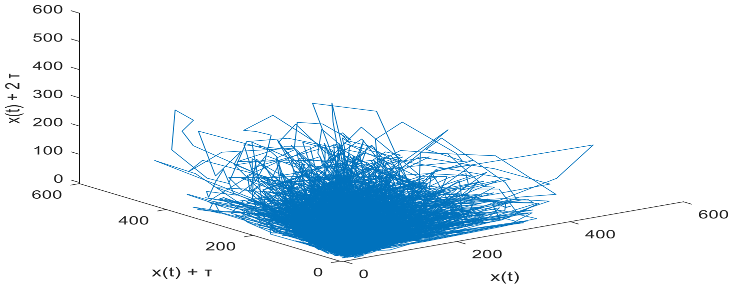

Figures 4: Phase space reconstruction for geomagnetic parameter (AE) during the solar maximum from January 1st to December 31st, 2014 (a) 2D reconstruction (b) 3D reconstruction.

a

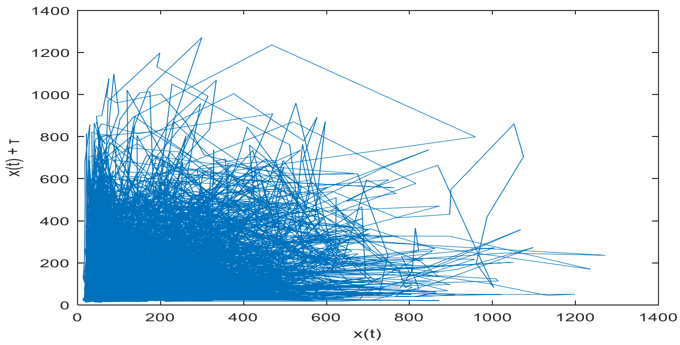

b

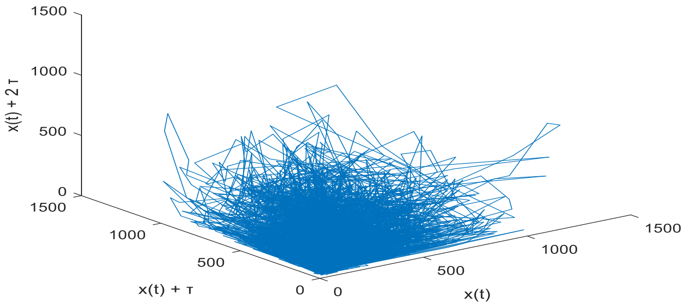

Figure 5: Phase space reconstruction for geomagnetic parameter (AU) during the solar maximum from January 1st to December 31st, 2014 (a) 2D reconstruction (b) 3D reconstruction.

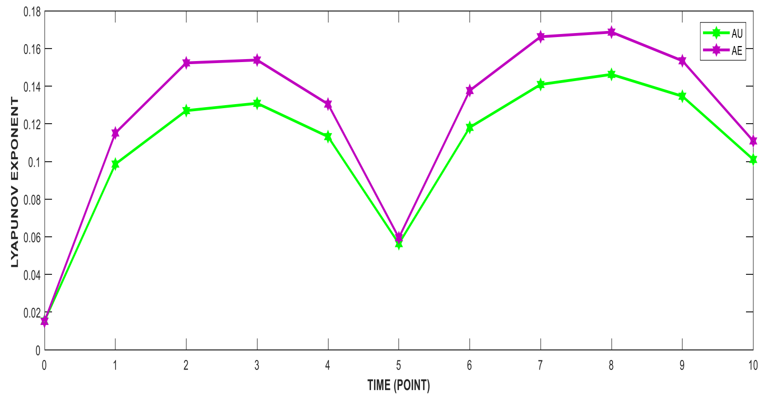

Figures 6: Lyapunov exponent for AU and AE during the solar maximum of the geomagnetic parameters from January 1st to December 31st, 2014.

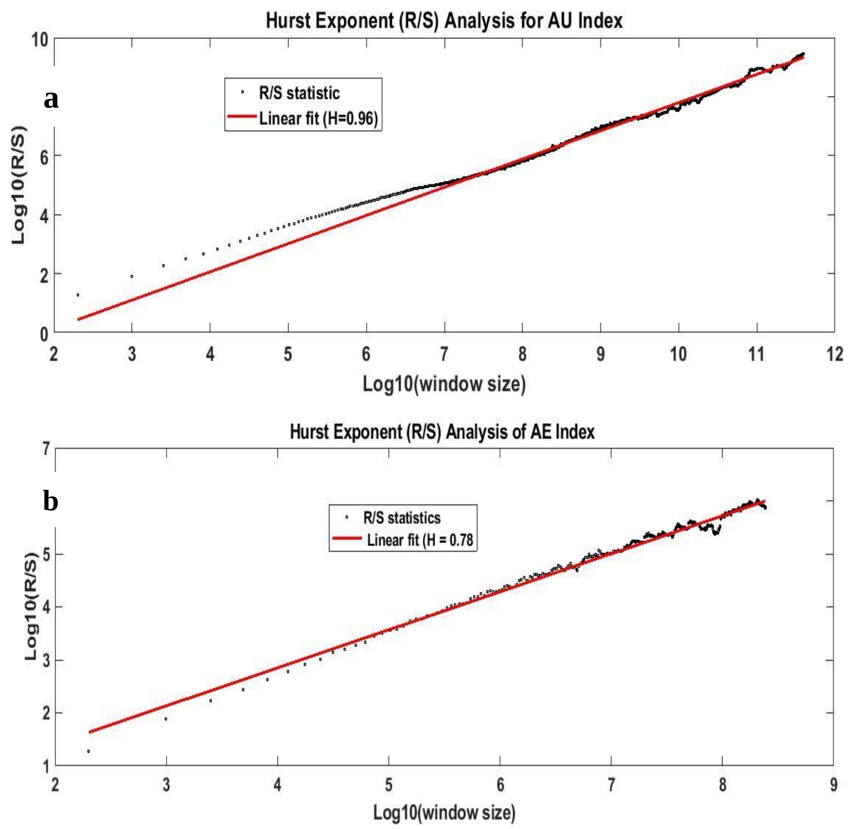

Figures 7: Hurst Exponent for geomagnetic parameter during the solar maximum from January 1st to December 31st, 2014 (a) AU and (b) AE

These abrupt and intermittent bursts in both indices correspond well with magnetospheric loading and unloading cycles that have been widely documented in earlier studies. Vassiliadis *et al.* (1995b) noted that AE contains deterministic bursts within a stochastic background, and Consolini and Chang (2001), described the geomagnetic system as evolving toward a critical state where magnetic energy accumulates and is released in avalanche-like bursts. The present study also align with Pavlos *et al.*(2012) that reported that AU typically exhibits larger amplitude variations due to its direct coupling with dayside ionospheric currents. Notably, the 2014 dataset demonstrates both frequent substorm events and quieter periods, indicating that geomagnetic activity is driven by a combination of solar wind forcing and internal magnetospheric dynamics.

A quantitative assessment of the geomagnetic data reveals that AE values exceed 500 nT approximately 12% of the time, whereas AU peaks above 700 nT for roughly 8% of the dataset. These proportions are slightly higher than those reported by Takalo *et al.*, (1994), suggesting a period of enhanced geomagnetic activity in 2014, possibly related to solar cycle conditions.

The nonlinear characteristics of the time series become even clearer when evaluating the Average Mutual Information (AMI). The AMI for both AE and AU exhibits a sharp initial decrease from lag 1 to lag 2, indicating that the strongest dependence between states occurs at very short time intervals. This rapid decay is clearly visible in Figure 2, where AMI drops steeply before tapering gradually at longer time delays making the choice of delay time $\tau = 12$. The slow, non-zero convergence of AMI implies the presence of long-range temporal dependencies, behaviour consistent with previous studies showing memory retention in geomagnetic indices.

This behaviour aligns with one of the previous studies. Takalo *et al. (1*994) demonstrated that geomagnetic indices retain memory of solar wind forcing over several hours, consistent with our observation of slow AMI decay. The rapid initial decay reflects the system's immediate response to fluctuations in the interplanetary magnetic field, while the long-term tapering implies persistence and memory effects across multiple temporal scales. Comparatively, AE demonstrates slightly shorter memory times than AU, which may reflect the more stochastic nature of substorm initiation compared to the quasi-periodic influence of dayside reconnection on AU. AS clearly sow as well in Figure 2, AMI also drops steeply before tapering gradually at longer time delays making the choice of delay time $\tau = 12$. This difference supports Vassiliadis *et al.* (1990), who observed that AU often exhibits stronger long-term correlations due to the sustained influence of solar wind–magnetosphere coupling.

The False Nearest Neighbours (FNN) analysis provides a direct view of the underlying dimensionality of the system. For both AE and AU, the proportion of false neighbours is high in dimensions one and two, gradually decreases through intermediate dimensions, and approaches near-zero at approximately the fifth to seventh dimensions. This progressive reduction is presented in Figure 3, where FNN percentages fall consistently across successive embedding dimensions with the first minimum at $m = 7$ for both AE and AU. These findings correspond closely with results reported by Vassiliadis *et al.* (1990). Pavlos *et al.*(2012), reported embedding dimensions for AE ranging between 5 and 8. The implication is that both proxies can be modeled with a state variable of seven (7) accurately. Figures 4(a) and 5(a) are phase space reconstruction in 2D projection for AE and AU respectively while 4(b) and 5(b) are phase space reconstruction in 3D projection for AE and AU respectively as well. Figures 4 and 5 therefore show that both solar proxies are chaotic in nature.

The behaviour of the Lyapunov exponent further clarifies the nature of this complexity. The Lyapunov spectrum derived for both AE and AU shows consistently positive values throughout the reconstruction as clearly depicted in Figure 6. These positive exponents reflect a high degree of sensitivity to initial conditions, confirming the behavior of both solar proxies of possessing characteristics of chaotic systems, meaning that very small differences in the present state can lead to significantly different future trajectories. Such sensitivity is typical of nonlinear magnetospheric processes driven by turbulent plasma flows, current disruptions, and variable solar wind–magnetosphere interactions. Eckmann and Ruelle (1985) emphasized that geomagnetic indices exhibit chaotic signatures, especially during active geomagnetic intervals. The slightly larger Lyapunov exponents observed for AU compared to AE suggest that the eastward electrojet may respond more strongly to short-lived variations in external forcing.

When synthesizing the outcomes from the time series, AMI, FNN, and Lyapunov analyses, it becomes evident that the AE and AU indices display a rich, nonlinear dynamical structure. The AMI in Figure 2 confirms both short-term memory and long-term correlations. The FNN results in Figure 3 demonstrate that the system evolves within a bounded low-dimensional attractor, confirming the presence of deterministic structure. The Lyapunov exponents in Figure 6 provide evidence that this deterministic structure is chaotic in nature, characterized by sensitivity to initial conditions and limited long-term predictability. Figures 7(a – b) revealed the Hurst Exponent values calculated for AU and AE indices time series data with the approximated values of 0.96 and 0.78 respectively. The results showed that AU and AE indices exhibit persistence nature.

Figures 8(a – b) show the variation of the AE and AU which depict the intensity of the geomagnetic storms patterns. It was noted that both AE and AU displayed similarly irregularities throughout the year 2014, the storms are more significant during the mid of the year for AE and AU with average powers of 16000mm^2 and 60000mm^2 respectively. The power showed that the severity of AU is more than AE. This indicates that the intensity of eastward ionospheric currents, reflecting the level of geomagnetic activity during substorms and magnetospheric disturbances are higher than the overall strength of the auroral electrojets currents flowing in the high-latitude ionosphere.

Overall, the nonlinear analysis presented in this study reveals that AE and AU indices are shaped by a deterministic yet chaotic dynamical system, with behaviour arising from the interplay of solar wind conditions, magnetotail storage processes, and ionospheric current dynamics. These insights demonstrate that traditional linear methods alone cannot fully capture the depth of geomagnetic

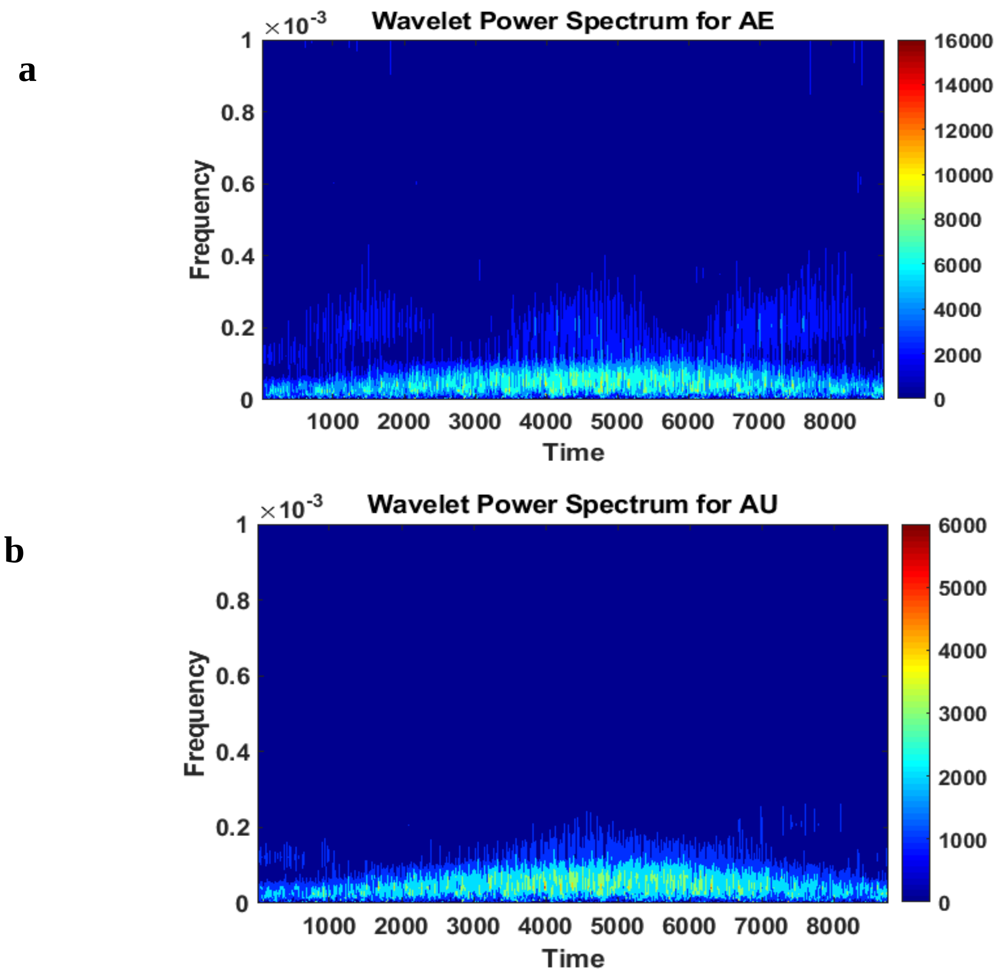

Figure 8: Wavelet Power Spectrum for geomagnetic parameters during the solar maximum from January 1st to December 31st, 2014 (a) AE and (b) AU.

variability, reinforcing the necessity of nonlinear analytical frameworks for understanding space weather phenomena and improving predictive modelling of geomagnetic disturbances. According to the results, the geomagnetic storm appears to be a linear system even though the magnetosphere, that generates it, has irregular characteristics (Unnikrishnan *et al.*, 2006a; Unnikrishnan *et al.*, 2006b; Falayi *et al* 2021). The combined impacts of internal magnetospheric activity and the solar wind could constitute the cause of the magnetosphere's unpredictable behavior (Unnikrishnan, 2010). Similarly, Earth's magnetosphere, which displays nonlinear structural extension, is greatly impacted by fluctuations in the magnetosphere-ionosphere system driven by the solar wind. It might be possible to minimize the internal variability of the magnetosphere system, which could cause the system to drift toward stochasticity instead of deterministic chaos (Bamidele *et al.*, 2025b). As stochastic drivers, solar winds have the ability to cause storms in the system, especially when coronal mass ejections (CMEs) appear and cause geomagnetic storms.

4.0 Conclusion

The study investigated the dynamics of AU and AE indices using both nonlinear dynamic time series techniques and wavelet spectrum analysis. The enhancement of the geomagnetic storms for AE and AU indices are more significant in the mid of the year 2014. The nonlinear analyses also demonstrate that the AE and AU indices exhibit deterministic structure with chaotic behaviour. The system evolves on a low-dimensional attractor, sensitive to initial conditions, and exhibits both short-term and long-range temporal correlations. These characteristics highlight the importance of using nonlinear approaches to understand, model, and predict magnetospheric dynamics and space weather phenomena that can be attributed to coronal mass ejections for the period of high solar activity.

References

Abarbanel, H. D. I., & Lali, R. (1996). *Analysis of observed chaotic data. New York, NY: Springer-Verlag.* 13 – 93.

Adelaja A. D., Laoye J.A., Odunaike R.K., Falayi E.O., Adeniji Q. A. & Ogunsanwo F. O. (2021). Study of Total Solar Irradiance Time Series using Chaotic Time Series and Wavelet Power Spectrum Analysis. *FUW Trends in Science & Technology Journal*. *6*(2), 408 – 414.

Adelaja A. D., Onma O. S., Idowu B. A., Opeifa S. T& Ogabi C. O. (2024). Jerk Chaotic System: Analysis, Circuit Simulation, Control and

Synchronization with Application to Secure Communication. Nigerian Journal of Theoretical and Environmental Physics, 2 (2), 56 – 69.

Albert, J. S., Destouni, G., Duke-Sylvester, S. M., Magurran, A. E., Oberdorff, T., Reis, R. E., & Ripple, W. J. (2021). Scientists' warning to humanity on the freshwater biodiversity crisis. *Ambio*, *50*(1), 85-94.

Alves, P. R. L., Duarte, L. G. S., & da Mota, L. A. C. P. (2017). A new characterization of chaos from a time series. *Chaos, Solitons & Fractals*, *104*, 323-326.

Ambika, G., & Harikrishnan, K. P. (2019). Methods of nonlinear time series analysis and applications: A review. *Dynamics and control of energy systems*, 9-27.

Balasis, G., Boutsi, A. Z., Papadimitriou, C., Potirakis, S. M., Pitsis, V., Daglis, I. A., Anastasiadis, A., & Giannakis, O. (2023). Investigation of Dynamical Complexity in Swarm-Derived Geomagnetic Activity Indices Using Information Theory. *Atmosphere*, *14*(5), 890.

Bamidele, K.J., Adelaja, A.D., Fowodu, T.O., Kotoye, A.A., Ajose, A.S., Falayi, F.C., Falayi., E.O. (2025a). Quantitative Analysis of Geomagnetic Indices Using Wavelet Power Spectrum. *Nigerian Journal of Environmental Sciences and Technology*, 9(1), pp. 86-104.

Bamidele, K.J, Falayi, E.O, Roy-Layinde, T.O, Adelaja, A.D., T.O. Fowodu and Falayi, F.C. (2025b): Chaos theory of geomagnetic indices during maximum year of 2014. *Basrah Journal of science*, 43(2), pp. 492- 520.

Chang, T. (1999). Self-organized criticality, multifractal spectra, and intermittent turbulence in the magnetotail. *Physics of Plasmas*, 6(11), 4137–4145.

Chen, G., Hsu, S. B., Huang, Y., & Roque-Sol, M. A. (2011). The spectrum of chaotic time series (II): wavelet analysis. *International Journal of Bifurcation and Chaos*, *21*(05), 1457-1467.

Consolini, G., & Chang, T. (2001). Dynamics of the magnetosphere: Complexity, self-organized criticality, and chaos. Space Science Reviews, 95(1-2), 87–100.

Davis, T. N., & Sugiura, M. (1966). Auroral electrojet activity index AE and its universal time variations. *Journal of Geophysical Research*, 71(3), 785–801. Eckmann, J.-P., & Ruelle, D. (1985). Ergodic theory of chaos and strange attractors. Reviews of Modern Physics, 57(3), 617–656.

Falayi, E. O., Ogundile, O. O., Adepitan, J. O., & Okusanya, A. A. (2019). Solar quiet variation of the horizontal and vertical components of geomagnetic field using wavelet analysis. *Canadian Journal of Physics*, *97*(4), 450-460.

Falayi, E.O., Adewole, A.T., Adelaja, A.D., Ogundile, A.A. & Roy-Layinde, T.O. (2020). Study of nonlinear time seriesand wavelet power spectrum analysis using solar wind parameters and geomagnetic indices. Nriag Journal of Astronomy and Geophysics. 9(1), 226–237.

Falayi, E. O., Ajose, A. S., Roy-Layinde, T. O., & Adewole, A. T. (2021). Analyzing the Variation of Lyapunov Exponents of the Time Derivatives of the Horizontal Geomagnetic Field during the Geomagnetic Storm.*Geomagnetism and Aeronomy*, *61*(8), 1221-1233.

Falayi, E. O., Amaechi, P. O., & Oluwafemi, J. A. (2024). Analysis of total electron content over the African low-latitude region during the maximum phase of solar cycle 24 (2012–2014). *Journal of Atmospheric and Solar-Terrestrial Physics*, *258*, 106235.

Farge, M. (1992). Wavelet transforms and their applications to turbulence. *Annual review of fluid mechanics*, *24*(1), 395-458.

Fraser, A. M., & Swinney, H. L. (1986). Independent coordinates for strange attractors from mutual information. Physical Review A, 33(2), 1134–1140.

Hirata, Y., Suzuki, H., Aihara, K., & Small, M. (2006). Estimating the time delay to reconstruct phase space using a global minimization algorithm. Physical Review E, 74(2), 026202.

Hurst, H. E. (1951). Long-Term Storage Capacity of Reservoirs. Transactions of the American Society of Civil Engineers *116*(1).0006518

Gómez-Águila, A., Trinidad-Segovia, J. E., & Sánchez-Granero, M. A. (2022). Improvement in Hurst exponent estimation and its application to financial markets. *Financial Innovation*, *8*(1), 86.

Ishii, M., Berdermann, J., Forte, B., Hapgood, M., Bisi, M. M., & Romano, V. (2024). Space weather impact on radio communication and navigation. A*dvances in Space Research*.

Kamide, Y., Baumjohann, W., Daglis, I. A., Gonzalez, W. D., Grande, M., Joselyn, J. A., & Vasyliunas, V. M. (1998). Current understanding of magnetic storms: Storm-substorm relationships. *Journal of Geophysical Research: Space Physics*, *103*(A8), 17705-17728.

Kennel, M. B., Brown, R., & Abarbanel, H. D. (1992). Determining embedding dimension for phase-space reconstruction using a geometrical construction. *Physical review A*, *45*(6), 3403.

Kivelson, M. G., Khurana, K. K., Russell, C. T., Walker, R. J., Warnecke, J., Coroniti, F. V., & Schubert, G. (1996). Discovery of Ganymede's magnetic field by the Galileo spacecraft. *Nature*, *384*(6609), 537-541.

Mallat, S. (1999). *A wavelet tour of signal processing*. Elsevier.

Meyers, S. D., Kelly, B. G., & O'Brien, J. J. (1993). An introduction to wavelet analysis in oceanography and meteorology: With application to the dispersion of Yanai waves. *Monthly weather review*, *121*(10), 2858-2866.

Mitra, S. K. (2012). Is Hurst exponent value useful in forecasting financial time series. *Asian social science*, *8*(8), 111-120.

Momeni, M., & Migoya-Orué, Y. (2025). Solar activity and ionospheric variation: A comprehensive study using hurst exponent and probability density functions analysis. *Advances in Space Research*, *75*(10), 7668-7683.

Nakamura, M., Yoneda, A., Oda, M., & Tsubouchi, K. (2015). Statistical analysis of extreme auroral electrojet indices. *Earth, Planets and Space*, *67*(1), 153.

Nikolopoulos, D., Moustris, K., Petraki, E., Koulougliotis, D., & Cantzos, D. (2019). *Fractal and Long-Memory Traces in PM10 Time Series in Athens, Greece. Environments*.

Ogunsua, B. O., Laoye, J. A., Fuwape, I. A., & Rabiu, A. B. (2014). The comparative study of chaoticity and dynamical complexity of the low-latitude ionosphere, over Nigeria, during quiet and disturbed days. *Nonlinear Processes in Geophysics*, *21*(1), 127-142.

Pavlos, G. P., Karakatsanis, L. P., Xenakis, M. N., & Athanasiou, M. (2012). Nonlinear dynamics of the geomagnetic AE index: Embedding dimension and determinism. Physica A: Statistical Mechanics and Its Applications, 391(5), 1601–1614.

Rabiu, A. B., Ogunsua, B. O., Fuwape, I. A., & Laoye, J. A. (2015). The transient variation in the complexes of the low-latitude ionosphere within the equatorial ionization anomaly region of Nigeria. *Nonlinear Processes in Geophysics*, *22*(5), 527-543.

Riabova, S. (2018). Application of wavelet analysis to the analysis of geomagnetic fieldvariations. Journal of Physics: Conference Series, Volum 1141, International Conference` on Mathematical Modelling in Physical Sciences 27–31 October 2018, Moscow, Russian. Federation.

Rostoker, G. (1972). Polar magnetic substorms. *Reviews of Geophysics*, *10*(1), 157-211.

Sarris, T. E. (2019). Understanding the ionosphere thermosphere response to solar and magnetospheric drivers: status, challenges and open issues. *Philosophical Transactions of the Royal Society A*, *377*(2148), 20180101.

Schreiber, T., & Kantz, H. (1995). Noise in chaotic data: Diagnosis and treatment. *Chaos: An Interdisciplinary Journal of Nonlinear Science*, *5*(1), 133-142.

Sharma, A. S., Vassiliadis, D., & Papadopoulos, K. (1993). Reconstruction of low-dimensional magnetospheric dynamics by singular spectrum analysis. Geophysical Research Letters, 20(5), 335–338.

Sierra-Porta, J.D., Petro-Ramos, D.J., Ruiz-Morales, D.D., Herrera-Acevedo, A.F. García-Teheran, M. Tarazona Alvarado. (2024). Machine learning models for predicting geomagnetic storms across five solar cycles using Dst index and heliospheric variables, *Advances in Space Research*, 74(8), 3483-3495.

Suresh, R., & Selvaraj, R. S. (2017). Nonlinear time series analysis of geomagnetic indices during geomagnetic storms. Advances in Space Research, 59(9), 2290–2302.

Takalo, J., Timonen, J., & Vassiliadis, D. (1994). Nonlinear characteristics of the AE index: Mutual information and attractor dimension. Journal of Geophysical Research, 99(A7), 13411–13424.

Takens, F. (1981). Lecture notes in mathematics. *by DA Rand and L.-S. Young Springer, Berlin*, *898*, 366.

Unnikrishnan, K., Balachandran, N., & Venugopal, C. (2006a). Nonlinear time series analysis of ionospheric variations during disturbed periods. Journal of Atmospheric and Solar-Terrestrial Physics, 68(12), 1422–1430.

Unnikrishnan, K., Balachandran, N., & Venugopal, C. (2006b). Chaotic behavior in ionospheric parameters during space weather disturbances. Annales Geophysicae, 24(10), 2589–2598.

Unnikrishnan, K. (2008). Comparison of chaotic aspects of magnetosphere under various physical conditions using AE index time series. In *Annales Geophysicae* 26(4), 941-953. Göttingen, Germany: Copernicus Publications.

Unnikrishnan, K. (2010). Characterization of geomagnetic storm time series using nonlinear techniques. Earth, Planets and Space, 62(6), 503–512.

Vassiliadis, D., Tattersall, J., Papadopoulos, K., & Sharma, A. S. (1990). Low-dimensional chaos in magnetospheric substorms. Geophysical Research Letters, 17(1), 109–112.

Vassiliadis, D., Sharma, A. S., Eastman, T. E., & Papadopoulos, K. (1995a). Low-dimensional chaos in magnetospheric activity from AE time series. Geophysical Research Letters, 22(21), 2681–2684.

Vassiliadis, D., Takalo, J., Papadopoulos, K., & Sharma, A. S. (1995b). Nonlinear dynamics of the AE index. Journal of Geophysical Research: Space Physics, 100(A1), 123–132.

Vlachos, I., & Kugiumtzis, D. (2009). Nonuniform state-space reconstruction and coupling detection. Physical Review E, 79(1), 016217.

Wanliss, E. (2005). Nonlinear Processes in Geophysics. Germany: European Geophysical Society.

Zbilut, J. P., & Webber Jr, C. L. (1992). Embeddings and delays as derived from quantification of recurrence plots. *Physics letters A*, 171(3-4), 199-203.